LATERAL STABILITY OF RAILWAY VEHICLES AND NEW CONTACT FORMULATIONS

Paulo R. R. de Campos, MSc Student

Debora N. Higa, MSc Student

Alfredo Gay Neto, Prof. Dr.

paulorrcampos@usp.br

debora.higa@usp.br

alfredo.gay@usp.br

Polytechnic School at the University of São Paulo

Av. Prof. Almeida Prado, travessa 2, 83, 05508-900, São Paulo, SP, Brazil

Abstract. *The present work has two main objectives: in the first part, classical governing equations for the lateral movement of a railway vehicle, developed by Carter in 1916, are introduced; its main hypotheses are discussed. In addition, the first method of Lyapunov is applied to determine the critical speed of a typical wheelset. Then, in the second part of the work, a rigid body model together with a contact formulation is employed to solve the same problem, namely "Master-Surface to Master-Surface Contact Formulation". Preliminary models are developed employing this new contact formulation and using simplified geometries. These models are intended to reproduce the so-called "hunting phenomenon", in a fully nonlinear environment. Although several further developments are required, the results are very promising.*

Keywords: *Railway Vehicles, Hunting, Master-Master Contact*

INTRODUCTION

Railway vehicles differ from others, because they operate on rails. The fundamental mechanism to guide these vehicles is the wheelset configuration, which, in summary, consists of two conical wheels, rigidly attached to an axle (Figure 1).

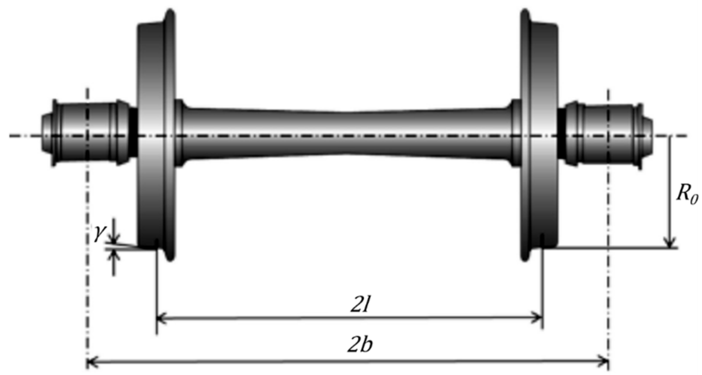

Figure 1 – Railway wheelset geometry. (TOURNAY, 2015)

On the one hand, the conicity of the wheels makes the vehicle orientation in curves easier, since it allows the experience of a difference in rolling radius between both wheels. On the other hand, the conicity may introduce lateral vehicle oscillations, called "hunting". This oscillation introduces forces into the system, which may cause vehicle and rail damage, discomfort to the passengers and even increase the risk of derailment. The longitudinal speed at which the vehicle becomes unstable is called critical speed and its determination is essential in railway vehicles design.

Hunting is nonlinear in its essence. Moreover, this phenomenon is a result from the coupling between the forces present in the very complex wheel-rail contact interface and the lateral and yaw movements of the bogie and its components. Nevertheless, some classic linearized models are available and can be used to provide a first insight into the phenomenon. The objective of this work is to study the "hunting" phenomenon through the classical Carter's equations and to try to develop preliminary railway models employing a novel contact technique, entitled master-surface to master-surface contact formulation.

An outline of the work is as follows: In section 1 the equations of motion, as proposed by Carter, are reviewed. In section 2 , the issue of determining critical speeds is addressed. Then, in section 3 , the recent master-master contact formulation is briefly introduced. At the end, numerical examples are developed in order to illustrate the applicability of the models.

1 EQUATIONS OF MOTION

The first realistic model of the lateral dynamics of a railway vehicle was that presented by Carter (1916, *apud* Wickens (2006)). Carter introduced the conicity of the wheel and the creepage in his model, which will be exposed below.

1.1 Geometry, freedoms and constrains

Two reference frames are defined to determine the wheelset and rail geometric parameters. The first $Oxyz$ lies on the centerline of the undistorted track and moves at the speed of the vehicle, V. Ox lies along the tangent to the track centerline, Oy lies in the radial direction of the curve and Oz is mutually perpendicular. The second reference frame $O^*x^*y^*z^*$ is fixed on the wheelset center of mass. O^*y^* lies on the axle centerline, O^*x^* and O^*z^* are mutually perpendicular as shown in Figure 2.

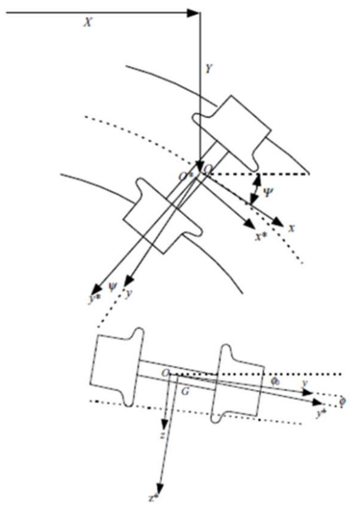

Figure 2 - Wheelset axis systems and coordinates. (WICKENS, 2005)

The track has curvature radius in the horizontal plane R_0, cross level ϕ_0 and a lateral displacement y_0. These values can vary along the track.

The rotations on the frame of reference $O^*x^*y^*z^*$ relatives to the axes O^*z^*, O^*x^* and O^*y^* are, respectively, the yaw ψ, the roll ϕ and the pitch θ.

The displacement of the wheelset center of mass relative to the set of axis $Oxyz$ is represented by the vector $x_0 = [u_x \, u_y \, u_z]$.

Since O^* is in the plane Oyz ($u_x = 0$) and assuming that the wheelset moves at constant speed V, the wheelset position and orientation can be defined by six variables: the lateral and vertical displacements u_y and u_z, the longitudinal position along the track $s = Vt$ and the rotations ψ, ϕ and θ.

Whereas the wheel and rail contact points and the angles made by the contact planes must be the same, and the bodies cannot penetrate each other, the contact point position is determined.

Proceedings of the XXXVIII Iberian Latin-American Congress on Computational Methods in Engineering
P.O. Faria, R.H. Lopez, L.F.F. Miguel, W.J.S. Gomes, M. Noronha (Editores), ABMEC, Florianópolis, SC, Brazil, November 5-8, 2017.

1.2 Creepage

Due to the rolling motion, an effect denominated creepage can occur at the contact patch. The deviation in relative velocity between the contact patch on the wheel and on the rail crown, divided by the forward speed of the wheelset is referred to as the longitudinal creepage. Similarly, lateral creepage is defined as the relative lateral velocity of the same contact patches divided by the forward speed. The relative angular motion between contact patches about the normal vector that describes the contact is referred to as spin creepage (WICKENS, 2005).

1.3 Equations of Motion

Assuming the hypothesis that the displacement components u_i and their derivatives are small and that the contact between the wheelset and the rails occurs at two points since the contact patch area is neglected as it is small compared to the dimensions of the track (this is usually referred as a "pointwise" approach to describe contact action), the equations of motion are derived applying the principles of linear and angular momentum and displacements and neglecting second order terms (see Wickens (2005) for detailed discussions), resulting in:

$$A\ddot{r} + F(r) = 0. \tag{1}$$

Where

$$r = [u_x \; u_y \; u_z \; \phi \; \chi \; \psi]^T. \tag{2}$$

$$A = diag[m \; m \; m \; I \; I_y \; I]. \tag{3}$$

And

$$F(r) = {}^cF + {}^gF + {}^wF + {}^fF + {}^nF + {}^sF. \tag{4}$$

m is the wheelset mass, I_i is the wheelset mass moment of inertia and ${}^cF$, ${}^gF$, ${}^wF$, ${}^fF$, ${}^nF$ and ${}^sF$ are, respectively, the centrifugal forces, gyroscopic forces, gravitational forces, creep forces, normal forces and the forces applied by the rest of the vehicle, given by:

$${}^cF = \left[0 \quad \frac{mV^2 cos\phi_0}{R_0} \quad -\frac{mV^2 sin\phi_0}{R_0} \quad \ddot{\phi}_0 \quad I_y V \frac{d}{dt}\left(\frac{sin\phi_0}{R_0}\right) \quad IV\frac{d}{dt}\left(\frac{cos\phi_0}{R_0}\right)\right]^T. \tag{5}$$

$${}^gF = \left[0 \quad 0 \quad 0 \quad \frac{I_y V\left(\dot{\psi} + V\frac{cos\phi_0}{R_0}\right)}{r_0} \quad 0 \quad -\frac{I_y V(\dot{\phi} + \dot{\phi}_0)}{r_0}\right]^T. \tag{6}$$

$${}^wF = [0 \quad -mgsin\phi_0 \quad -mgcos\phi_0 \quad 0 \quad 0 \quad 0]^T. \tag{7}$$

$${}^fF + {}^nF = [-T_x \quad -T_y \quad -T_z \quad -M_x \quad -M_y \quad -M_z]^T. \tag{8}$$

$${}^sF = [P_x \quad P_y \quad P_z \quad L_\phi \quad L_\theta \quad L_\psi]^T. \tag{9}$$

Where T_i and M_i are the efforts acting on the wheelset as shown in Figure 3, and P_i and L_i are the efforts transmitted by the suspension.

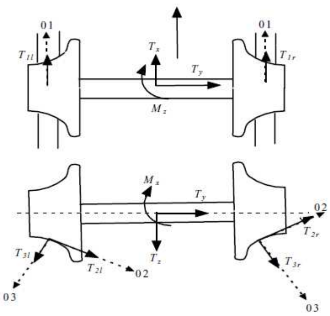

Figure 3 – Efforts acting on the wheelset. (WICKENS, 2005)

However, the actual motion of the railway wheelset is constrained; the wheels remain in contact with the track at two points and the wheelset is assumed to be at a constant speed V relative to an axis system fixed in the earth. Thereby, two of the coordinates are eliminated. Furthermore, vertical displacement and roll angle can be assumed to be dependent functions of lateral displacement and yaw.

Hence a new set of generalized coordinates q_θ, q_y and q_ψ is defined representing the motions in which there is no normal displacement of the contact area as the normal deflections are small compared to the total motion of the wheelset, then:

$$\begin{bmatrix} u_x \\ u_y \\ u_z \\ \phi \\ \theta \\ \psi \end{bmatrix} = \begin{bmatrix} 0 & 0 & 0 \\ 0 & 1 & 0 \\ 0 & z_y & 0 \\ 0 & \phi_y & 0 \\ 1 & 0 & 0 \\ 0 & 0 & 1 \end{bmatrix} \begin{bmatrix} q_\theta \\ q_y \\ q_\psi \end{bmatrix}, \tag{10}$$

or

$$\boldsymbol{r} = \boldsymbol{J}\boldsymbol{q}. \tag{11}$$

Where:

$$\phi_y = \frac{d\phi}{du_y}, \tag{12}$$

$$z_y = \frac{du_z}{du_y}. \tag{13}$$

Substituting (11) in (1), considering z_y and ϕ_y are dependent on q_y and neglecting small terms in comparison with the other terms according to practical values, the system is reduced to three equations of motion (with three degrees of freedom).

For small displacements, e. g., assuming a very small amplitude motion, the equation system can be linearized, obtaining a system with two generalized coordinates, q_y and q_ψ, that will be described, respectively, by y and ψ.

Taking into account the creepages, considering that ϕ_0 and the contact slopes are small and that the wheel radius r_0 is negligible compared to the radius of the curve R_0, the equation of motion can be written by:

$$m\ddot{y} + 2f_{22}\frac{\dot{y}}{V} - 2f_{22}\psi + \left(\frac{2f_{23}}{V} - \frac{I_y\kappa V}{r_0 l}\right)\dot{\psi} + \left[k_y + \frac{2N_0\varepsilon_0^*}{l} - \frac{2\varepsilon_0^*}{l}\frac{f_{23}}{r_0}\right]y = Q_y. \tag{14}$$

$$I_z\ddot{\psi} - \left(\frac{2f_{23}}{V} - \frac{I_y\delta_0 V}{r_0 l}\right)\dot{y} + \frac{2f_{11}l^2}{V}\dot{\psi} + \frac{2f_{11}\lambda_0 l}{r_o}y + [k_\Psi - 2N_0 l\delta_0 + 2f_{23}]\psi = Q_\psi. \tag{15}$$

Where l is half of the distance between the two contact points, f_{ij}'s are the ratio between the creep force and the creepage evaluated with the wheelset central, N_0 and δ_0 are the normal force and the angle made by the contact plane with the horizontal,

$m\ddot{y}$ and $I_z\ddot{\psi}$ represent the inertial terms,

$\frac{2f_{22}}{V}\dot{y}$, $\frac{2f_{23}}{V}\dot{\psi}$, $\frac{2f_{23}}{V}\dot{y}$ and $\frac{2f_{11}l^2}{V}\dot{\Psi}$ represent the creep damping terms,

$\frac{2\varepsilon_0^*}{l}\frac{f_{23}}{r_0}y$, $-2f_{22}\psi$, $\frac{2f_{11}\lambda_0 l}{r_o}y$ and $2f_{23}\psi$ represent the creep stiffness or terms,

$-\frac{I_y\kappa V}{r_0 l}\dot{\psi}$ and $\frac{I_y\delta_0 V}{r_0 \mathrm{l}}\dot{y}$ represent the gyroscopic terms,

$\frac{2N_0\varepsilon_0^*}{l}y$ and $-2N_0 l\delta_0\psi$ represent the gravitational stiffness effects,

k_y and k_ψ represent the elastic suspension (lateral and yaw spring stiffness action) and

Q_y and Q_ψ are the generalized applied forces.

With null externally applied forces and for a restrained wheelset, the parameters that compose the contact stiffness terms (creep and gravitational stiffness) are very small compared to the lateral and yaw spring stiffness k_ψ and k_y. Therefore, one may neglect these terms giving the simplified equation of motion:

$$m\ddot{y} + 2f_{22}\frac{\dot{y}}{V} - 2f_{22}\psi + k_y \mathrm{y} = 0. \tag{16}$$

$$I_z\ddot{\psi} + \frac{2f_{11}l^2}{V}\dot{\psi} + \frac{2f_{11}\lambda_0 l}{r_o}\mathrm{y} + k_\psi\psi = \frac{2f_{11}l}{R_o}. \tag{17}$$

2 CRITICAL SPEEDS

Wheel conicity is the main feature of the self-guiding mechanism in a railway vehicle. However, it is also one of the characteristics that introduce lateral oscillations in the system, the so called "hunting phenomenon" – that plays a role even in straight tracks, due to system imperfections. Lateral oscillation observed during hunting introduces additional forces into the system. If not controlled, this behavior can result in very serious consequences, such as discomfort to passengers, vehicle and rail damage or, in a worst scenario, derailment.

The speed for which lateral oscillation becomes unstable is called "critical speed". According to Tournay (2015), in summary, the following conditions are predicted with respect to the critical speed:

- Below critical speed, hunting amplitude decreases.
- At the critical speed, amplitude of the motion remains constant.
- Above critical speed, hunting amplitude increases.

Determining critical speeds is an essential task in the design of railway vehicles. In this section, we propose a technique to determine critical speeds when assuming Carter's equations of motion.

2.1 Lyapunov's first method

We now introduce the first, or indirect, Lyapunov method. For a comprehensive discussion on stability theory and Lyapunov methods, please refer to Leipholz (1987).

Recalling the governing equations derived by Carter, but now assuming tangent (straight) track ($R_o \to \infty$):

$$m\ddot{y} + 2f_{22}\left(\frac{\dot{y}}{V} - \psi\right) + k_y y = 0. \tag{18}$$

$$I_z\ddot{\psi} + \frac{2f_{11}l^2}{V}\dot{\psi} + \frac{2f_{11}\gamma l}{r_o}y + k_\psi \psi = 0. \tag{19}$$

The first step of the method consists of reducing Eq. (18) and (19) into a first order system by introducing state variables, as follows:

$$x_1 = y, \;\; x_2 = \psi, \;\; x_3 = \dot{y}, \;\; x_4 = \dot{\psi}. \tag{20}$$

So that

$$\dot{x}_1 = x_3, \;\; \dot{x}_2 = x_4, \;\; \dot{x}_3 = \ddot{y}, \;\; \dot{x}_4 = \ddot{\psi}. \tag{21}$$

Proceedings of the XXXVIII Iberian Latin-American Congress on Computational Methods in Engineering
P.O. Faria, R.H. Lopez, L.F.F. Miguel, W.J.S. Gomes, M. Noronha (Editores), ABMEC, Florianópolis, SC, Brazil, November 5-8, 2017.

Then, Eq. (18) and (19) can be rewritten as:

$$\ddot{y} = -\frac{1}{m}\left(2f_{22}\left(\frac{\dot{y}}{V} - \psi\right) + k_y y\right). \tag{22}$$

$$\ddot{\psi} = -\frac{1}{I_z}\left(\frac{2f_{11}\gamma l y}{r_o} + \frac{2f_{11}l^2\dot{\psi}}{V} + k_\psi \psi\right). \tag{23}$$

In matrix form, we have:

$$\dot{\boldsymbol{x}} = \boldsymbol{A}\boldsymbol{x} \rightarrow \begin{Bmatrix} \dot{x}_1 \\ \dot{x}_2 \\ \dot{x}_3 \\ \dot{x}_4 \end{Bmatrix} = \begin{bmatrix} 0 & 0 & 1 & 0 \\ 0 & 0 & 0 & 1 \\ -\frac{k_y}{m} & \frac{2f_{22}}{m} & -\frac{2f_{22}}{mV} & 0 \\ -\frac{2f_{11}\gamma l}{I_z r_o} & -\frac{k_\psi}{I_z} & 0 & -\frac{2f_{11}l^2}{I_z V} \end{bmatrix} \begin{Bmatrix} x_1 \\ x_2 \\ x_3 \\ x_4 \end{Bmatrix}. \tag{24}$$

One can extract the eigenvalues of matrix $\boldsymbol{A}$, and the Lyapunov theorem states that:

- If all eigenvalues of $\boldsymbol{A}$ have negative real part, i.e., $Re_k < 0$, then the state is said to be Lyapunov-Stable.
- On the other hand, if at least one of the eigenvalues of $\boldsymbol{A}$ has a positive real part, i.e., $Re_k > 0$, then the state is said to be Lyapunov-Unstable.
- Finally, if $Re_k = 0$, the state is said to be Lyapunov-Critical.

These steps can be applied in a straightforward manner to determine the critical speed of a railway vehicle, as exemplified further in this work.

3 CONTACT FORMULATION

In this work, we very briefly describe the main characteristics of the so called master-surface to master-surface contact formulation. The genesis of this contact formulation is based in an approach for beam-to-beam contact – in finite element context, as presented in 1997 (WRIGGERS, et al., 1997). The main peculiarity of such formulation is that it does not assume, from beginning, a distinction between master and slave bodies, as commonly done in the context of computational contact mechanics – particularly when performing a node-to-surface approach (details may be found extensively in (WRIGGERS, 2006)). Recently, the technique was generalized into a "master-surface to master-surface" general pointwise contact formulation, by using super-elliptical parameterized surfaces (GAY NETO, et al., 2016) and (GAY NETO, et al., 2017).

This work is not intended to develop the mathematical aspects of master-master contact formulation, for that purpose, readers may refer to the above-mentioned original references.

In Figure 4, two surfaces candidate to contact are illustrated, namely $\mathbf{\Gamma}_{\mathrm{A}}$ and $\mathbf{\Gamma}_{\mathrm{B}}$.

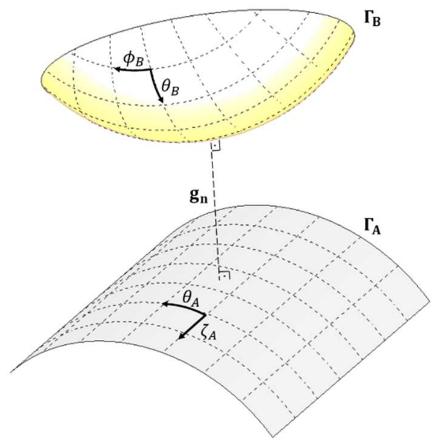

Figure 4 – Parameterized surfaces candidate to contact. (DE CAMPOS, et al., 2017)

As mentioned before, the main characteristic of the master-master contact formulation, which makes it eminently different from traditional methods such as the master-slave approach, is that there is no need to elect any slave point in one of the surfaces. In other words, both surfaces are treated as master-surfaces, which means that both surfaces are parameterized using convective coordinates. Convective coordinates can be understood as material coordinates that are attached to the surface, and then, that deform with the surface.

Since both surfaces are parameterized, one can establish the normal gap vector function, $\mathbf{g}_{\mathrm{n}} = \mathbf{\Gamma}_{\mathrm{A}} - \mathbf{\Gamma}_{\mathrm{B}}$, illustrated in Figure 4. Furthermore, by imposing orthogonality conditions and assuming a pointwise interaction, the contacting point can be found through optimization processes or by employing a Newton-Raphson root finder for 4-variable functions, as extensively discussed by Gay Neto, et al. (2016). For convex surfaces, the solution can be obtained straightforwardly, since a good initial guess is chosen, which may be developed for each kind of surface parameterization, accordingly.

In the tangential direction, Coulomb's constitutive law for friction is assumed. Moreover, the master-master contact formulation is based on the fully redefinition of the tangential gap function, as discussed by Gay Neto, et al. (2017). In roughly words, tangential gap redefinition is needed to account for the rigid body rotation present, for example, in a rolling scenario, i.e., the rigid body rotation effect is built-in the gap function.

With both gap functions defined, one can develop the weak form and the tangent operator for the contact contribution to the global solution of a nonlinear finite element formulation. Distinct approaches can be used to impose the contact constraints. The master-master contact formulation, as originally proposed by Gay Neto, et al. (2016), employs the penalty technique.

The principal advantage of the master-master contact formulation is that once the minimum distance problem is solved, i.e., once the contacting point is obtained for a given configuration of the surfaces, only one gap function has to be evaluated for each contact pair. When compared with traditional approaches, where multiple gap functions have to be evaluated, this feature implies in a reduction of computational costs. However, the main hypothesis, that can represent a drawback of the formulation, is the pointwise assumption. By this, a mechanically equivalent point load is used to represent the contact action. Despite being a limitation, we highlight that the pointwise assumption is satisfactory for several important cases from engineering, e.g., wheel-rail interface, ball bearings and many others.

4 NUMERICAL EXAMPLES

In this section, examples are developed to illustrate the practical application of the methods presented in this work. A typical wheelset is analyzed when operating on tangent tracks, the main characteristics of the model is presented in Table 1. Carter's equations were implemented in Wolfram *Mathematica*® language and NDSolve function (WOLFRAM, 2017) was used for time integration. Moreover, using the same program, stability analyses were performed using the first method of Lyapunov. Next, some very preliminary models are developed in a nonlinear finite environment - GIRAFFE platform (GAY NETO, 2017). These models employ the master-surface to master-surface contact formulation in a try to reproduce the hunting phenomenon using simplified geometries and modern computational methods.

Table 1. Railway wheelset properties (WICKENS, 2005)

Typical measures for a railway vehicle		
$m = 1250\text{kg}$	$f_{11} = 7.44\text{MN}$	$k_y = 0.23\text{MN/m}$
$I_z = 700\text{kg.m}^2$	$f_{22} = 6.79\text{MN}$	$k_\psi = 2.5\text{MN.m/rad}$
$r_o = 0.45\text{m}$	$\gamma = 0.1174$	$l = 0.7452\text{m}$

4.1 Carter's equations and the first method of Lyapunov

With the characteristics provided in Table 1, one can calculate matrix $\boldsymbol{A}$ from Eq.(24) and then, a very simple routine can be developed to find the critical speed, as follows:

1. Define a starting (null) value for velocity, $V = 0.0\text{m/s}$
2. Define an increment for the calculations. For example, define $inc = 0.01$ for obtaining critical speeds with a precision of two decimal places.
3. Extract eigenvalues of $\boldsymbol{A}$ for the current value of V.
4. Check if $Re_k \geq 0,\ with\ k = 1, 2, 3\ and\ 4$.
5. If all eigenvalues have negative real part, increase the current value of V by inc and repeat the process from step 3 to step 5. Otherwise, stop the calculation and evaluate the current value of V, it will represent the critical speed.

By performing these five steps for the model proposed in Table 1, the critical speed for this vehicle is found to be 74.26m/s (267.3km/h).

Once the critical speed is known, one can check if the conditions predicted in Section 2 are observed in practice. To do that, we performed time integration of Carter's equations considering an initial lateral offset of 0.01m. Results are shown for cases below critical speed, at critical speed and above critical speed (Figure 5, Figure 6 and Figure 7, respectively).

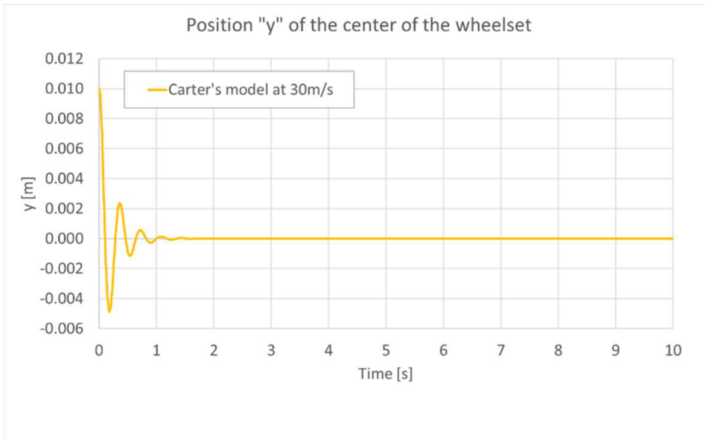

Figure 5 – Time evolution of lateral displacements, y, for an initial lateral offset of 0.01m. Below critical speed: $V = 30.0\text{m/s}$.

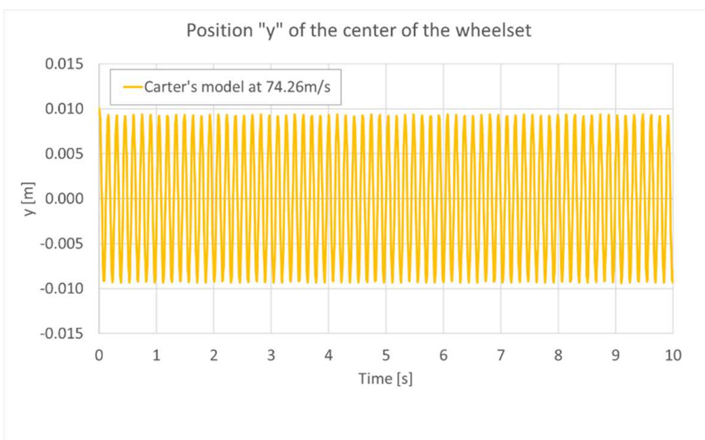

Figure 6 – Time evolution of lateral displacements, y, for an initial lateral offset of 0.01m. At critical speed: $V = 74.26\text{m/s}$.

Proceedings of the XXXVIII Iberian Latin-American Congress on Computational Methods in Engineering
P.O. Faria, R.H. Lopez, L.F.F. Miguel, W.J.S. Gomes, M. Noronha (Editores), ABMEC, Florianópolis, SC, Brazil, November 5-8, 2017.

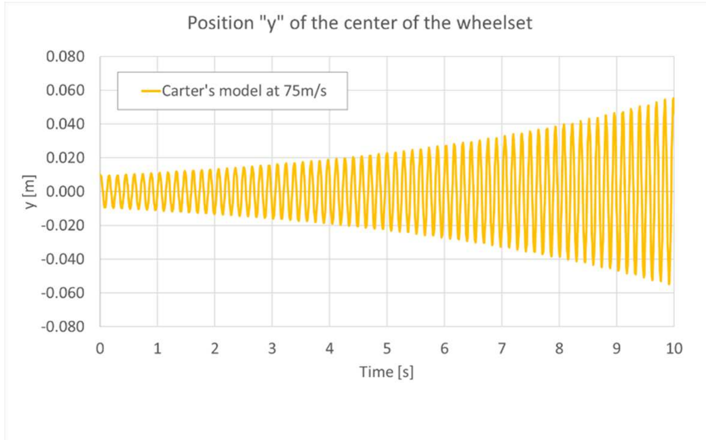

Figure 7 – Time evolution of lateral displacements, y, for an initial lateral offset of 0.01m. Above critical speed: $V = 75.0\text{m}/s$

4.2 Nonlinear model with master-master contact

In this section, we present a very preliminary model employing the master-surface to master-surface contact formulation into the study of hunting phenomenon. In Figure 8, the nonlinear model used in conjunction with the master-master contact formulation is shown. Figure 8 (a) presents an overview of the model. A rigid body is defined at point 1, this element is free to move in any direction, except from longitudinal direction (x), which has an imposed constant forward speed. Contact surfaces are shown in green: rails are idealized as rigid beams with circular cross section with radius of 0.04m and the rigid wheel profile is depicted in Figure 8 (b).

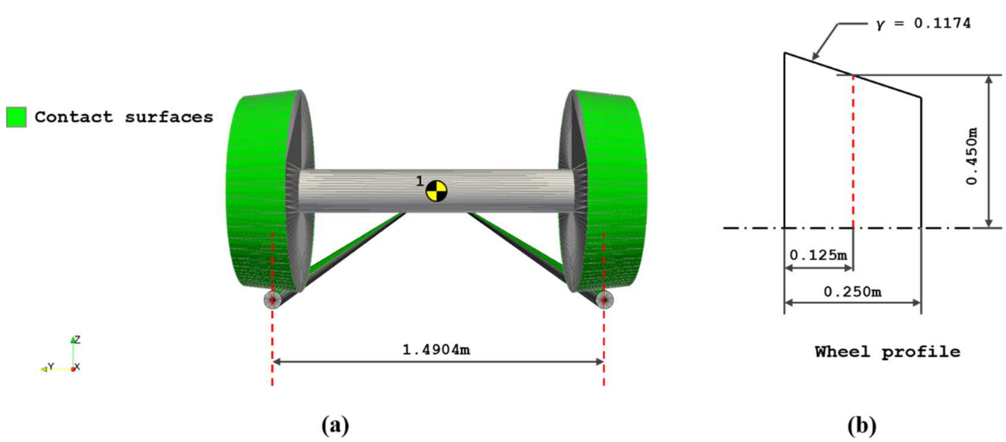

Figure 8 – Nonlinear model: (a) General overview of wheelset model. (b) Wheel profile dimensions.

Proceedings of the XXXVIII Iberian Latin-American Congress on Computational Methods in Engineering
P.O. Faria, R.H. Lopez, L.F.F. Miguel, W.J.S. Gomes, M. Noronha (Editores), ABMEC, Florianópolis, SC, Brazil, November 5-8, 2017.

The rigid body shown in Figure 8 has the same properties of the model of Table 1. In addition, since it is a 3D model, it was necessary to define $I_x = 700\text{kg.m}^2$ and $I_y = 115\text{kg.m}^2$. A constant load of 78480N (4 tonnes per wheel) was applied. Carter's model (WICKENS, 2005) does not use a coefficient of friction explicitly. Indeed, linear creepages from Kalker's linear theory (f_{11} and f_{22}) are assumed. At this moment, only Coulomb's friction law is available in Giraffe and therefore a coefficient of friction, $\mu = 0.3$ was adopted in our nonlinear model. Moreover, in the current release of Giraffe (GAY NETO, 2017), it is not possible to represent lateral and yaw stiffness (k_y and k_ψ). Assuming null stiffness for both parameters drastically reduces the critical speed. Actually, the model becomes unstable for any velocity in such scenario.

To obtain some reasonable results, we performed a simulation for a constant speed of 15m/s. Although this is much lower than the critical speed predicted in the previous section, since we are assuming $k_y = k_\psi = 0$, unstable behavior is expected.

At this point, it is worth mentioning that there exist a very important difference between the Coulomb's friction law (used in Giraffe) and the linear creepage theory (used together with the Carter's model). In Figure 9 (a), classical Coulomb's frictional behavior is illustrated: once the tangential forces are above a certain limit (proportional to the compressive normal contact force, $F_N \leq 0$, and the friction coefficient, μ) then the contacting surfaces start (suddenly) sliding. On the other hand, Figure 9 (b) illustrates the concept of creepage, which is a kind of regularization of the stick-slip condition. Moreover, the linear creepage model employed in Carter's model does not saturate friction, that is, there is no upper-bound for friction forces.

In fact, to avoid the non-differentiability of the Coulomb's law, in numerical procedures the tangential constraint is imposed by techniques such as the penalty method. The penalty factor ε_T used to impose the tangential constraint can notably influence the overall behavior of the model. While very high penalty factors impose conditions such as that illustrated in Figure 9 (a), if penalty factors are relaxed, the condition illustrated in Figure 9 (c) is obtained. Notice that Figure 9 (c) is similar in some sense to Figure 9 (b).

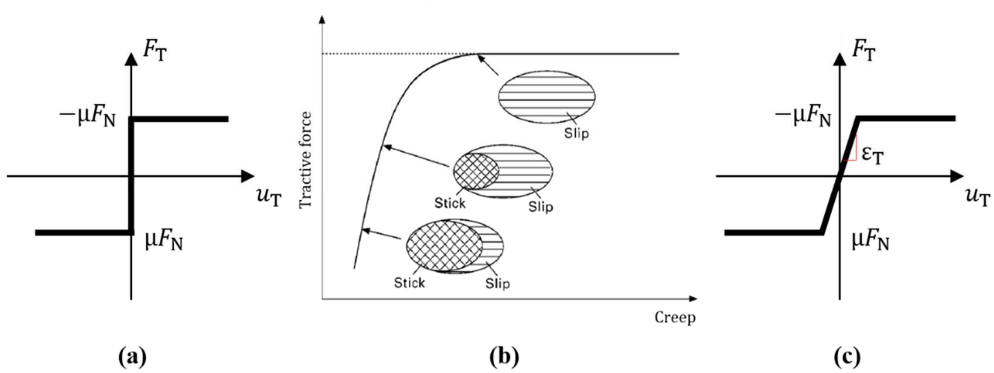

Figure 9 – Frictional behavior. (a) Coulomb's law. (b) Creepage concept. (c) Coulomb's law in a penalty approach. Adapted from (WRIGGERS, 2006) and (TOURNAY, 2015)

For the model described above, we performed three analyses varying the tangential penalty factor. The normal penalty factor was kept constant between different models ($\varepsilon_N =$

1.0E8N/m). Table 2 summarizes the model properties and the results are shown in figure Figure 10.

Table 2. Nonlinear models

Model	$\boldsymbol{\varepsilon_N}$ **[N/m]**	$\boldsymbol{\varepsilon_T}$ **[N/m]**	$\boldsymbol{V}$ **[m/s]**
WS01		1.0E7	
WS02	1.0E8	1.0E8	15
WS03		1.0E9	

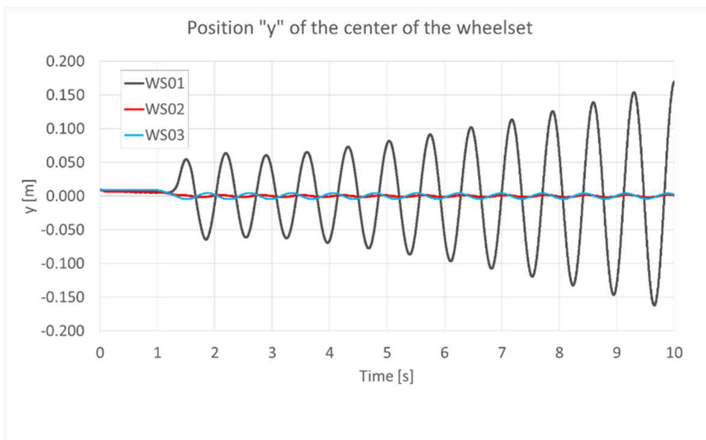

Figure 10 – Nonlinear model response: time evolution of lateral displacements for different tangential penalty factors. Speed: $\boldsymbol{V = 15.0 m/s}$

Then, for the same model, the tangential penalty factor was calibrated in order to obtain results similar to those predicted by Carter's equation at a speed of 15m/s. A model identified as WS04 was generated, and $\varepsilon_T = 3.6E7 N/m$ was employed for that. Comparative results are shown in Figure 11.

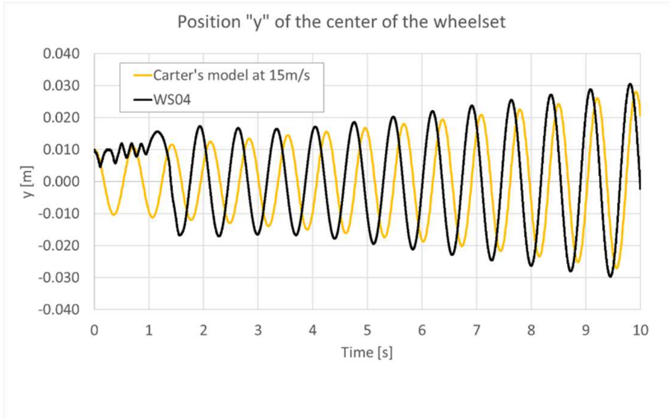

Figure 11 – Nonlinear model response: time evolution of lateral displacements for $\varepsilon_T = 3.6E7 N/m$. Speed: $V = 15.0 m/s$

CONCLUSIONS

In this work, the so-called hunting phenomenon was studied. Classical linear equations of motion, developed by Carter in 1916, were applied to study the lateral behavior of a typical wheelset. Moreover, the first method of Lyapunov was presented as a very simple and efficient way to define critical speeds for such kind of model. Responses relative to the critical speed obtained via Lyapunov's first method is in accordance with the expected behavior: amplitude of lateral movement increases above the critical speed and decreases below it.

Furthermore, the contact formulation entitled master-surface to master-surface was briefly reviewed and applied to the railway case. Although this contact formulation provides several advantages in terms of computational efficiency, it was observed that employing the Coulomb's friction law directly, with no creepage in pre-saturation regime, may not be adequate to reproduce the hunting phenomenon. The overall behavior of the wheelset is very sensitive to the choice of the tangential penalty factor. We have shown that by relaxing this factor, we tend to obtain responses similar to those predicted by the Carter's model. However, it is very difficult to calibrate penalty factors properly.

For future works, we highlight the need of developing suspension elements, in order to consider the effects of k_y and k_ψ. In addition, it is clearly necessary to combine the master-master contact formulation with friction laws more elaborated than only the Coulomb's one, but compound it with physical insights due to flexibility of contacting bodies to evaluate creepage coefficients (e.g., by Kalker's theory). Both themes are ongoing research topics of the authors.

ACKNOWLEDGEMENTS

The authors would like to acknowledge Vale S.A. for the support through Wheel-Rail Chair project and Altair Brazil, for providing full access to the HyperWorks suite. The third author also acknowledges CNPq (Conselho Nacional de Desenvolvimento Científico e Tecnológico) under the grant 308190/2015-7.

REFERENCES

DE CAMPOS P. R. R. and GAY NETO A. Master-surface to master-surface contact formulation applied to rigid-flexible multibody systems [Conference] // 5th International Conference on Computational Contact Mechanics, ICCCM 2017. - Lecce : [s.n.], 2017.

GAY NETO A. Giraffe User's Manual v.1.0.173 – Generic Interface Readily Accessible for Finite Elements [Online]. - 2017. - 08 17, 2017. - http://sites.poli.usp.br/p/alfredo.gay/GIRAFFE%20User's%20Manual%20v1.0.173.pdf.

GAY NETO A., PIMENTA P. M. and WRIGGERS P. A Master-Surface to Master-Surface Formulation for Beam to Beam Contact. Part I: Frictionless Interaction [Journal] // Comput. Methods Appl. Mech. Engrg.. - 2016. - http://dx.doi.org/10.1016/j.cma.2016.02.005.

GAY NETO A., PIMENTA P. M. and WRIGGERS P. A Master-Surface to Master-Surface Formulation for Beam to Beam Contact. Part II: Frictional Interaction [Journal] // Comput. Methods Appl. Mech. Engrg.. - 2017. - Vol. 319. - pp. 146-174. - http://dx.doi.org/10.1016/j.cma.2017.01.038.

LEIPHOLZ H. Stability Theory [Book]. - Stuttgart : Springer Fachmedien Wiesbaden, 1987. - 2.

TOURNAY H. The Fundamentals of Vehicle/Track Interaction [Book Section] // Guidelines to Best Practices For Heavy Haul Railway Operations: Management of the Wheel and Rail Interface / book auth. International Heavy Haul Association. - Virginia : Simmons-Boardman Books, Inc., 2015.

WICKENS A. H. A History of Railway Vehicle Dynamics [Book Section] // Handbook of Railway Vehicle Dynamics / ed. IWNICK Simon. - Boca Raton : CRC Press, 2006.

WICKENS A. H. Fundamentals of Rail Vehicle Dynamics: Guidance and Stability. [Book]. - Lisse : Swets & Zeitlinger Publishers, 2005.

WOLFRAM Advanced Numerical Differential Equation Solving in the Wolfram Language [Online]. - 2017. - 08 17, 2017. - https://reference.wolfram.com/language/tutorial/NDSolveOverview.html.

WRIGGERS P. and ZAVARISE G. On contact between three-dimensional beams undergoing large deflections [Journal] // Commun. Numer. Methods Eng.. - 1997. - Vol. 13. - pp. 429-438.

WRIGGERS P. Computational Contact Mechanics [Book]. - New York : Springer-Verlag Berlin Heidelberg, 2006. - 2.